

1 **Contrasting the Direct Radiative Effect and Direct Radiative Forcing of Aerosols**

2
3 **C. L. Heald^{1,2}, D. A. Ridley¹, J. H. Kroll¹, S. R. H. Barrett³, K. E. Cady-Pereira⁴, M. J. Alvarado⁴, C. D. Holmes⁵**

4
5 [1] {Department of Civil and Environmental Engineering, Massachusetts Institute of
6 Technology, Cambridge, MA, USA }

7 [2] {Department of Earth, Atmospheric and Planetary Sciences, Massachusetts Institute of
8 Technology, Cambridge, MA, USA }

9 [3] {Department of Aeronautics and Astronautics, Massachusetts Institute of Technology,
10 Cambridge, MA, USA }

11 [4] {Atmospheric and Environmental Research (AER), Lexington, MA, USA }

12 [5] {Department of Earth System Science, University of California, Irvine, CA, USA }

13 Correspondence to C.L. Heald (heald@mit.edu)

14 15 **Abstract**

16 The direct radiative effect (DRE) of aerosols, which is the instantaneous radiative impact of all
17 atmospheric particles on the Earth's energy balance, is sometimes confused with the direct
18 radiative forcing (DRF), which is the change in DRE from pre-industrial to present-day (not
19 including climate feedbacks). In this study we couple a global chemical transport model (GEOS-
20 Chem) with a radiative transfer model (RRTMG) to contrast these concepts. We estimate a
21 global mean all-sky aerosol DRF of -0.36 Wm^{-2} and a DRE of -1.83 Wm^{-2} for 2010. Therefore,
22 natural sources of aerosol (here including fire) affect the global energy balance over four times
23 more than do present-day anthropogenic aerosols. If global anthropogenic emissions of aerosols
24 and their precursors continue to decline as projected in recent scenarios due to effective pollution
25 emission controls, the DRF will shrink (-0.22 Wm^{-2} for 2100). Secondary metrics, like DRE,
26 that quantify temporal changes in both natural and anthropogenic aerosol burdens are therefore
27 needed to quantify the total effect of aerosols on climate.

29 **1 Introduction**

30 Atmospheric aerosols are the most uncertain driver of global climate change (IPCC, 2013).
31 These particles can scatter or absorb radiation, thereby cooling or warming the Earth and its
32 atmosphere directly. They also play a pivotal role in cloud formation, acting as nuclei for liquid
33 or ice water clouds, and can thus indirectly cool the planet by increasing its albedo. The overall
34 impact of present-day atmospheric aerosols is estimated to be a cooling, globally
35 counterbalancing a significant fraction of the warming associated with greenhouse gases (IPCC,
36 2013). There is thus a critical need to better quantify the role of aerosols in the climate system.
37 The ability of aerosols to modify climate depends on their atmospheric abundance over time as
38 well as their chemical, physical, and optical properties; uncertainties on all of which are large
39 (Myhre et al., 2013; Kinne et al., 2006).

40 The direct radiative effect (DRE) is Earth's instantaneous radiative flux imbalance between
41 incoming net solar radiation and outgoing infrared radiation resulting from the presence of a
42 constituent of the Earth's atmosphere (Boucher and Tanre, 2000). This is distinct from direct
43 radiative forcing (DRF), a leading climate-relevant metric for aerosol (and other constituents),
44 commonly used to quantify aerosol impacts (e.g. (Shindell et al., 2009)) and in international
45 assessment (e.g. (IPCC, 2013)). Generally, DRF quantifies the change in DRE over time which
46 will induce a change in global temperatures. In the context of the IPCC climate assessments, this
47 time horizon has been specified as pre-industrial (1750) to present-day (IPCC, 1990, 1995, 2001,
48 2007, 2013). In this IPCC framework, the radiative forcing has also been restricted to "denote an
49 externally imposed perturbation" (IPCC, 2001), and so excludes feedbacks resulting from a
50 changing climate itself. Both of these more specific definitions of radiative forcing have been
51 widely adopted by the atmospheric science and climate communities. The most recent IPCC
52 report (IPCC, 2013) also describes an alternate Effective Radiative Forcing (ERF), which allows
53 physical variables (e.g. the temperature profile) "to respond to perturbations with rapid
54 adjustments"; this does not generally include feedbacks or responses to climate change, but in
55 the case of aerosols, now includes the "semi-direct effect". The DRF includes both
56 anthropogenic forcing driven by the rise in human emissions and land-use change as well natural
57 forcing associated with changes in solar flux and volcanic emissions. This was not clear in a
58 previous definition of aerosol forcing in Section 2.4 of the 2007 IPCC report: "the direct RF only
59 considers the anthropogenic components." There are very few natural aerosol forcers, with

60 volcanoes, which are sporadic in nature and therefore difficult to compare with other forcers, as
61 the primary example. However, anthropogenic land use change and anthropogenically-driven
62 changes in the chemical environment can both affect natural aerosols, thus constituting a forcing
63 ignored by this second, incomplete definition.

64 Climate feedbacks can also drive changes in natural aerosols; for example rising
65 carbonaceous aerosol emissions associated with enhanced fire activity (Spracklen et al.,
66 2009;Westerling et al., 2006), the impacts of CO₂ fertilization on aerosol precursor emissions
67 (Heald et al., 2009), increases in biogenic aerosol formation associated with temperature-driven
68 increases in biogenic VOC emissions (Tsigaridis and Kanakidou, 2007;Heald et al., 2008), or
69 trends in dust emissions associated with changes in vegetation or wind speed (Mahowald et al.,
70 2006;Ridley et al., submitted). Carslaw et al. (2010) suggest that changes in natural aerosols,
71 largely driven by climate feedbacks may result in radiative perturbations of up to $\pm 1 \text{ Wm}^{-2}$.
72 Previous studies have attempted to differentiate the role of climate feedbacks on biogeochemical
73 cycles and atmospheric chemistry (Raes et al., 2010;Carslaw et al., 2010), however these
74 investigations require characterization of the climate response via a coupled chemistry-climate
75 model.

76 The DRF metric is relatively simple to estimate in atmospheric models (in that it does not
77 require quantification of the climate response) and enables quantitative comparison of various
78 anthropogenic forcing mechanisms on the Earth's energy budget. The aerosol DRF reflects both
79 the change in primary aerosol emissions from anthropogenic activity and the impacts of the
80 changing chemical environment (due to anthropogenic emissions) on secondary aerosol
81 formation. The radiative impacts of natural aerosol are typically reflected in DRE, not DRF.
82 Observations (from satellite or surface sunphotometers) characterize a total DRE of present-day
83 aerosols; to estimate DRF the anthropogenic fraction is assumed (Yu et al., 2006;Bellouin et al.,
84 2005). Indeed, as a result of this, observational studies such as Bellouin et al. (2013) have
85 provided a clear contrast between DRE and DRF. Nevertheless, this distinction between DRE
86 and DRF is sometimes confused in the literature (Jo et al., 2013;Heald et al., 2005;Liao et al.,
87 2004;Kim et al., 2006;Artaxo et al., 2009;Massoli et al., 2009;Ma et al., 2012;Athanasopoulou et
88 al., 2013;Goto et al., 2008), where the presence of any aerosol is assumed to imply a DRF. The
89 radiative imbalance associated with the presence of these aerosols is only a DRF if pre-industrial
90 concentrations were zero. However, the distinction between DRE and DRF remains somewhat

91 murky, particularly when considering secondary aerosol formation. For example, changes in the
92 chemical formation of biogenic secondary organic aerosol (SOA) due to changes in
93 anthropogenic nitrogen oxide (NO_x) emissions qualifies as a DRF, but similar changes induced
94 by changes in lightning NO_x sources (due to a climate feedback) do not. In this study our
95 objective is to globally quantify and contrast these two metrics.

96

97 **2 Model Description**

98 Reducing the uncertainty associated with aerosol radiative forcing requires models that are
99 well-tested against observations and that include the capacity to simulate radiative impacts. The
100 temporal matching of observations and simulation, which is only possible using a chemical
101 transport model (CTM) driven by assimilated meteorology (or a GCM nudged towards analyzed
102 meteorology), is critical to the accurate evaluation of a simulation of short-lived species.
103 Therefore, a CTM with an online coupled radiative transfer model is the most appropriate model
104 configuration for consistently evaluating aerosol loading and direct radiative impacts.

105 Here we integrate the fast radiation model RRTMG online within the global GEOS-Chem
106 chemical transport model (www.geos-chem.org), a configuration referred to as GC-RT, to
107 calculate the radiative fluxes associated with atmospheric aerosols. RRTMG uses the correlated-
108 k method to calculate longwave (LW) and shortwave (SW) atmospheric fluxes. Further details
109 on the aerosol simulation, emissions, optical properties, RRTMG, and the implementation in
110 GEOS-Chem are provided in what follows.

111

112 **2.1 GEOS-Chem**

113 We use v9-01-03 of GEOS-Chem driven by GEOS-5 assimilated meteorology from the
114 Global Model and Assimilation Office for the year 2010 at a horizontal resolution of 2°×2.5° and
115 47 vertical levels.

116 The GEOS-Chem oxidant-aerosol simulation includes H₂SO₄-HNO₃-NH₃ aerosol
117 thermodynamics coupled to an ozone-NO_x-hydrocarbon-aerosol chemical mechanism (Park et
118 al., 2004; Park et al., 2006). We use the standard bulk aerosol scheme, where all aerosols are
119 described with one or more log-normal size bins. The ISORROPIA II thermodynamic
120 equilibrium model (Fountoukis and Nenes, 2007) calculates the partitioning of total ammonia
121 and nitric acid between the gas and particle (fine mode only) phases. The model scheme also

122 includes organic aerosol (OA) and black carbon (BC) (Park et al., 2003), sea salt aerosol (2 size
123 bins) (Alexander et al., 2005;Jaegle et al., 2010), and soil dust (4 size bins) (Fairlie et al.,
124 2007;Ridley et al., 2012). The organic matter to organic carbon ratio for primary organic aerosol
125 (POA) is assumed to be 2. SOA is produced from the oxidation of biogenic hydrocarbons
126 following the Chung and Seinfeld (2002) 2-product model scheme, with the addition of isoprene
127 SOA (Henze and Seinfeld, 2006) and aromatic SOA (Henze et al., 2008). Of these three
128 categories of SOA, only yields for SOA formed from aromatic precursors include a dependence
129 on nitrogen oxide (NO_x) concentrations. Note that the anthropogenic SOA (and the DRF
130 associated with it) in GC-RT is only that formed from aromatic species. The soil dust simulation
131 uses the source function of Ginoux et al. (2004) and an entrainment scheme following the DEAD
132 model (Zender et al., 2003). Wet deposition of soluble aerosols and gases includes contributions
133 from scavenging in convective updrafts, rainout, and washout (Liu et al., 2001). Aerosol dry
134 deposition follows the size-dependent scheme of Zhang et al. (2001).

135 Global anthropogenic emissions for 2010 are based on the year 2000 EDGAR v3.2 inventory
136 (Olivier et al., 2001) for SO_x , NO_x and CO, and the RETRO inventory (Schultz, 2007) for VOCs.
137 BC and primary OC emissions are taken from Bond et al.(2007). Both natural and
138 anthropogenic (largely agricultural) ammonia emissions follow the global inventory of
139 Bouwman et al. (1997) with seasonal variation specified by Park et al. (2004). Global
140 anthropogenic emissions are over-written by regional inventories as described by van Donkelaar
141 et al. (2008). We scale all regional and global anthropogenic emissions from their respective base
142 year to 2006, the last year of available statistics (van Donkelaar et al., 2008). We use global
143 biomass burning emissions from the monthly GFED3 inventories (van der Werf et al., 2010).
144 Emissions associated with biofuel use and agricultural waste, are globally fixed (Yevich and
145 Logan, 2003) with seasonality but no interannual variability. Biogenic VOC emissions are
146 predicted interactively in GEOS-Chem using the MEGAN2 scheme (Guenther et al., 2006).
147 Emissions of DMS, NO_x from lightning and soils, dust, and sea salt depend on meteorology and
148 are computed online in the model as described by Pye et al., (2009). Tropospheric methane
149 concentrations are fixed at 2007 values from the NOAA CCGC cooperative air sampling
150 network (4 latitude bands, mean concentrations ranging from 1733 to 1856 ppb).

151 Anthropogenic emissions of ozone and aerosol precursors (SO_x , NO_x , NH_3 , BC, OC, CO, and
152 VOCs) for the year 2100 follow the RCP 4.5 scenario as implemented by Holmes et al. (2013).

153 These include fossil fuel, biofuel and agricultural emissions; all other natural and fire emissions,
154 as well as methane concentrations, are identical in the 2100 and 2010 simulations performed
155 here. We note that projections of aerosol precursor emissions show similar trajectories in all four
156 of the RCP scenarios, with the exception of ammonia which is projected to remain reasonably
157 constant in the RCP 4.5 scenario but projected to rise in all other scenarios. Global emission
158 totals for aerosols and their precursors in 2010 and 2100 are given in Table 1.

159 Recent versions of the GEOS-Chem standard aerosol simulation have been extensively tested
160 against airborne (van Donkelaar et al., 2008;Heald et al., 2011;Wang et al., 2011), shipborne
161 (Lapina et al., 2011), and surface site (Zhang et al., 2012;Heald et al., 2012) mass concentration
162 measurements as well as aerosol deposition measurements (Fisher et al., 2011) and satellite and
163 ground-based observations of AOD (Ridley et al., 2012;Jaegle et al., 2010;Ford and Heald,
164 2012).

165

166 **2.2 Rapid Radiative Transfer Model for GCMs (RRTMG)**

167 RRTMG (Iacono et al., 2008) is a fast radiative transfer code that calculates longwave and
168 shortwave atmospheric fluxes using the correlated-k method (Lacis and Oinas, 1991). The
169 absorption coefficients that are used to develop the code's k-distributions are attained directly
170 from the Line-By-Line Radiative Transfer Model (LBLRTM) (Clough et al., 1992;Clough et al.,
171 2005;Alvarado et al., 2013), which connects the spectroscopic foundation of RRTMG to high-
172 spectral resolution validations done with atmospheric radiance observations. There are 16 bands
173 in the longwave RRTMG code and 14 bands in the shortwave code (extending from 230 nm
174 through 56 μm); for boundaries see Mlawer et al.(1997) and Mlawer and Clough (1998).
175 Modeled sources of extinction in RRTMG include H_2O , O_3 , long-lived greenhouse gases,
176 aerosols, ice and liquid clouds, and Rayleigh scattering. RRTMG has been successfully
177 incorporated into a number of GCMs (Iacono et al., 2003;Iacono et al., 2008), including the
178 ECMWF IFS, the NCEP GFS and the NCAR CAM5.

179 For cloudy cases, vertical overlap of cloudy layers is handled using the Monte-Carlo
180 Independent Column Approximation (McICA; (Pincus et al., 2003)), which reduces the
181 computational load for the treatment of complex vertically overlapping cloud to that of a model
182 run for a simpler configuration (*e.g.* clear, single-layer clouds) by assigning statistically
183 appropriate combinations of cloud layers to each spectral element in the calculation. This

184 requires that comparisons between RRTMG and observed fluxes and heating rates average a
185 sufficiently large number of data points (in space and/or time) to remove the unbiased noise
186 introduced by the McICA approximation. This random noise in the radiative fluxes and heating
187 rates introduced by McICA has been shown to have statistically insignificant effects on GCM
188 simulations (*e.g.* (Barker et al., 2008)).

189 RRTMG has been shown to be highly accurate in tests against reference radiative transfer
190 calculations as part of the Continual Intercomparison of Radiation Codes (CIRC) project
191 (Oreopoulos and Mlawer, 2010; Oreopoulos et al., 2012), which included numerous evaluations
192 of the radiative effects due to aerosols.

193

194 **2.3 Integration of GEOS-Chem and RRTMG (GC-RT)**

195 RRTMG is called at a user-specified temporal frequency (3 hours here) within GEOS-Chem
196 and calculates instantaneous radiative fluxes in both the shortwave and longwave. In addition to
197 total fluxes, GC-RT can calculate the SW or LW flux associated with a specific constituent of
198 the troposphere (ozone, methane, sulfate, nitrate, ammonium, BC, OA, sea salt, dust or total
199 particulate matter) by calling RRTMG again with zero constituent concentration for the species
200 of interest and differencing the result. We describe the specification of a suite of relevant surface
201 and atmospheric composition properties here.

202 All aerosols in GEOS-Chem are treated as externally mixed with log-normal size
203 distributions and optical properties (including refractive indices and hygroscopic growth factors)
204 defined by the Global Aerosol Data Set (GADS) database (Kopke et al., 1997), with recent
205 updates (Drury et al., 2010; Jaegle et al., 2010; Ridley et al., 2012). We do not include any
206 absorption enhancement from the coating of BC in these simulations. We update the BC density
207 and refractive index to follow recommendations of Bond and Bergstrom (2006) and the
208 shortwave refractive indices for dust following Sinyuk (2003). We also link simulated sulfate
209 with the GADS water-soluble-type aerosol properties, not the sulfuric acid properties previously
210 applied in the GEOS-Chem simulation, as recommended by Hess et al. (1998). Table 2 gives the
211 relevant optical and size properties for dry aerosol. Mie code is used to calculate the resulting
212 optical properties (including mass extinction efficiency) at 7 discrete relative humidities (RH) for
213 each wavelength. The optical properties generated at 61 GADS wavelengths (from 250 nm to 40
214 μm) are spline interpolated to the 30 RRTMG wavelengths (230 nm to 56 μm) and stored in a

215 look-up table which includes the mass extinction efficiency, the single scattering albedo (SSA)
216 and asymmetry parameter (g). Aerosol properties at the two RRTMG wavelengths that fall
217 outside of the range of the GADS wavelengths are fixed at the values of the shortest and longest
218 wavelengths in GADS. The AOD at a specific wavelength is calculated within GEOS-Chem as a
219 function of local relative humidity from the mass concentration and mass extinction efficiency
220 according to the formulation of Tegen and Lacis (1996). RRTMG uses the AOD, SSA and
221 asymmetry parameter for each aerosol type to calculate aerosol impacts on radiative fluxes in
222 both the shortwave and longwave.

223 Vertical profiles of a suite of greenhouse gases are fixed in GC-RT for both longwave and
224 shortwave flux calculations. These include: N_2O and stratospheric CH_4 (following the July 2012
225 zonal mean climatology from the TES instrument), CFCs (CFC-11, CFC-12, and CCl_4 from
226 UARS climatology and CFC-22 from the MIPAS climatology, all scaled to match surface values
227 provided in IPCC (2007)) and CO_2 (set to 390 ppm globally). Zonally averaged tropospheric
228 methane concentrations are fixed as described in Section 2.1. Tropospheric ozone is simulated
229 interactively in GEOS-Chem; stratospheric concentrations are calculated based on the method
230 used in FAST-J (Wild et al., 2000). Water vapor concentrations are specified according to the
231 GEOS-5 assimilated meteorology. All gas-phase optical properties follow HITRAN (Rothman et
232 al., 2005), as described by Iacono et al (2008) and Mlawer and Clough (Mlawer and Clough,
233 1998).

234 Cloud optical properties required in RRTMG are calculated based on the liquid and ice
235 visible optical depths from the GEOS-5 assimilated meteorology. We assume fixed effective
236 radii of $14.2 \mu m$ for water droplets and $24.8 \mu m$ for ice particles based on a near-10-year average
237 of MODIS-Aqua data (L. Oreopoulos, personal communication). From the optical depths and
238 radii, we calculate the liquid and ice water path (LWP, IWP), the later based on the Fu (1996)
239 treatment of ice cloud particles. The optical properties (extinction, SSA and asymmetry
240 parameter) are then calculated from the L/IWP, the effective radii and a series of wavelength-
241 specific parameters for liquid water (Hu and Stamnes, 1993) and ice (Fu, 1996;Fu et al., 1998).
242 Bosilovich et al. (2011) provide an overview of the water budget in the MERRA re-analysis
243 (based on the same GEOS-5 assimilation system used here).

244 A climatology of surface albedo and emissivity is based on the multi-wavelength 8-day land
245 composites from MODIS for 2002 through 2007 available at 0.05° horizontal resolution (Schaaf

246 et al., 2002;Wan et al., 2002). The MODIS land emissivity product (MOD11C2) provided at 6
247 longwave wavelengths is interpolated to the 16 RRTMG wavelengths (values at wavelengths
248 outside of the observed range are held fixed at the edge values). The emissivity of the ocean is
249 set to 0.98. From Sidran (1981) this appears to be relatively constant between 0.2 μ m and 12 μ m,
250 after which it decreases slightly to 0.95 until beyond 40 μ m. The broadband direct and diffuse
251 albedos for both the UV-visible and visible-IR are specified from the MODIS land albedo data
252 (MCD43C3). Ocean albedo is held constant at 0.07 across all wavelengths (Stier et al., 2007).
253 We do not include diurnal variation in surface albedos. Annual mean surface albedos used here
254 are shown in Figure 1. We note that aerosols produce a very modest warming in the shortwave
255 over the most highly reflective hot spots over North Africa (El Djouf, Erg of Bilma and Great
256 Sand Sea), the Middle East, and Greenland (Figure 1).

257

258 **2.4 GC-RT Simulations**

259 To characterize the radiative impact of present-day aerosols we perform two simulations: a
260 baseline 2010 simulation and a second identical simulation with zero anthropogenic emissions
261 (biomass burning emissions are not included as anthropogenic, see details in Section 3). We zero
262 out anthropogenic emissions for 1750 following Dentener et al.(2006) who suggest that fossil
263 fuel emissions are negligible for this time period. We neglect here the biofuel emissions for
264 1750, which are small for carbonaceous aerosols (12% of present-day emissions) and negligible
265 for all other species according to Dentener et al. (2006). The difference between these
266 simulations provides an estimate of the anthropogenic contribution to the burden, AOD and
267 ultimately the DRF (which is defined under a fixed climate). While DRF for greenhouse gases is
268 calculated at the tropopause after stratospheric temperature adjustment, “for most aerosol
269 constituents, stratospheric adjustment has little effect on the RF, and the instantaneous RF at
270 either the top of the atmosphere or the tropopause can be substituted” (IPCC, 2007). Estimates of
271 the anthropogenic fraction of global dust emissions due to agricultural activities (e.g. plowing,
272 grazing, irrigation) vary widely (e.g. (Tegen et al., 2004;Mahowald and Luo, 2003)); here we
273 assume that 20% of all dust is of anthropogenic origin; the anthropogenic contribution likely
274 varies regionally, we assume a fixed fraction here.

275

276

277 3 Results

278 Table 3 summarizes the GC-RT aerosol simulation and compares these results to the
279 AeroCom I and AeroCom II model means where available (Myhre et al., 2013; Kinne et al.,
280 2006). Global annual mean burdens for OA and dust are similar (within 20% and 15%
281 respectively) to the model medians from the AeroCom I models for the year 2000 (Kinne et al.,
282 2006), whereas, the GC-RT burden of BC is about half of the AeroCom I model median value.
283 Koch et al. (2009) show that the AeroCom I models are on average a factor of 8 times larger than
284 BC concentrations measured aboard aircraft over the Americas, but underestimate BC at high
285 Northern latitudes and in Asia. Schwarz et al. (2010) show that the AeroCom I models generally
286 overestimate BC (by an average a factor of 5) in remote regions based on comparisons with the
287 HIPPO airborne observations over the Pacific. Sulfate is also 32% lower than the AeroCom I
288 median; however the sum of inorganic aerosol (sulfate, nitrate and ammonium) in GEOS-Chem
289 is within 5% of the sulfate-only value for AeroCom I. The burden of sea salt is significantly
290 lower (~40%) than AeroCom I, however the sea salt in GEOS-Chem has recently been evaluated
291 and refined based on comparisons with satellite and in situ observations (Jaegle et al., 2010). The
292 calculated global mean mass extinction efficiency (MEE) for all aerosol are lower than the
293 AeroCom II model means, however the wide range of model estimates given by Myhre et al.
294 (2013) suggests that these are not well constrained in the AeroCom II models. In fact this large
295 range in model MEE suggests that differences in model treatments of aerosol removal, size, and
296 optical properties (including water uptake) can lead to at least a factor of two difference in model
297 estimates of aerosol radiative fluxes.

298 Lower aerosol MEE in GC-RT translate to a lower global mean mid-visible AOD of 0.092
299 compared to the AeroCom I model mean of 0.127 and satellite-based estimates (~0.15) (Kinne et
300 al., 2006). Figure 2 shows the geographical distribution of annual mean AOD for present-day,
301 over half of which is attributed to dust and sea salt. Sulfate and OA contribute a further 33%,
302 with nitrate, ammonium and BC making minor near-source contributions to the global AOD. The
303 GC-RT anthropogenic AOD is 77% of the mean of the AeroCom II models. Similarly, the GC-
304 RT estimate of clear-sky (-0.57 Wm^{-2}) global mean TOA aerosol direct radiative forcing (DRF)
305 is 15% lower (less cooling) than the AeroCom II model mean.

306 The IPCC (2007) estimates the aerosol DRF at -0.5 Wm^{-2} (with a range of -0.9 to -0.1 Wm^{-2})
307 in 2005 based on both models and satellite measurement. The model-only value (adjusted for

308 dust and nitrate which is not included in all models) is lower at -0.4 Wm^{-2} . Our global-mean all-
309 sky value for 2010 (-0.36 Wm^{-2}) is similar. If we double BC absorption, as a crude
310 approximation of internal mixing, then the 2010 DRF would be -0.28 Wm^{-2} , a 20% change from
311 our base estimate. We do not include any biomass burning sources in our DRF calculation due to
312 the uncertainty in attributing the anthropogenic fraction. Anthropogenic modulation of biomass
313 burning emissions is driven by changing agricultural practices, land clearing, and human fire
314 suppression but not by climate change (this constitutes a feedback). We use an additional
315 simulation to estimate a DRE of -0.19 Wm^{-2} from all biomass burning particles in 2010 (-0.23
316 Wm^{-2} from OA, $+0.06 \text{ Wm}^{-2}$ from BC and -0.02 Wm^{-2} from inorganic aerosol). The IPCC (2007)
317 estimate of the aerosol DRF of biomass burning linked with human activities is $+0.03 \text{ Wm}^{-2}$,
318 indicating that the net impact of biomass burning aerosol is treated as more absorbing than our
319 estimate or that the amount and spatial distribution of the aerosol relative to underlying reflecting
320 clouds and areas with high surface albedo differ.

321 All-sky DRF in GC-RT is 63% of the estimate of clear-sky DRF. The global annual mean
322 cloud fraction in GC-RT for 2010 is 60%. This implies a global-mean cloud-sky TOA DRF of -
323 0.22 Wm^{-2} , a lower value (less cooling), consistent with a shading of scattering aerosols below-
324 clouds and enhanced absorption from BC above clouds. The all-sky to clear-sky ratio is typically
325 $\sim 50\%$ for the AeroCom II models (Myhre et al., 2013). Our slightly higher fraction is likely the
326 result of the lower estimated BC loading.

327 Table 3 shows that the total TOA radiative effects are dominated by aerosol impacts in the
328 shortwave (visible-UV) wavelengths, where they reflect solar radiation and cool the Earth (with
329 the exception of BC which absorbs solar radiation). Modest warming ($<10\%$ of the cooling
330 effect) results from scattering (by large particles such as dust) or absorption in the longwave (IR)
331 wavelengths (Figure 2). This indicates that a SW-only aerosol DRE estimate would overestimate
332 the cooling effect by $\sim 5\text{-}10\%$.

333 Figure 3 contrasts the GC-RT estimates of all-sky DRF and DRE. The DRF represents a
334 change in radiative balance from pre-industrial to present-day (2010) with fixed climate, which
335 reflects the rise in anthropogenic emissions (and anthropogenic land use, not considered here).
336 Conversely, the DRE represents the total present-day radiative impact from all aerosols in the
337 atmosphere, including those of natural origin. As a result, aerosols that are dominated by
338 anthropogenic sources (e.g. nitrate) show a similar DRE and DRF, whereas natural aerosols (e.g.

339 sea salt) have a large DRE but zero DRF. The estimate of total aerosol DRE (-1.83 Wm^{-2}) is
340 more than 5 times the value of the DRF (-0.36 Wm^{-2}) in 2010, thus the global radiative impact of
341 “natural” aerosol is more than 4 times that of anthropogenic aerosol perturbation. Rap et al.
342 (2013) estimated an all-sky natural aerosol DRE of -0.81 Wm^{-2} from DMS-sulfate, sea-salt,
343 terpene SOA and wildfire alone.

344 Figure 4 shows the zonal distribution of the GC-RT simulated radiative impacts. We see that
345 the forcing is highly concentrated at Northern mid-latitudes, driven by anthropogenic emissions
346 in North America, Europe and Asia, in agreement with previous model studies (Myhre et al.,
347 2013). Modest radiative impacts in the Arctic are the result of spring/summer Eurasian sulfate
348 pollution, during seasons of minimum snow cover. Conversely, the DRE is distributed
349 throughout the world with maxima associated with not only anthropogenic emissions in the NH,
350 but also with sea salt emissions in the Southern Ocean, biomass burning in the tropics and Arctic,
351 and dust from Africa and Asia. Warming dominates over the deserts in the Sahara, the Middle
352 East and the highly reflective regions at high Northern latitudes; shortwave scattering prevails in
353 all other regions in the simulation.

354 Similarly, Figure 5 shows that the global mean DRF from aerosols is largest in boreal
355 springtime (due to sulfate), whereas the DRE is more uniform throughout the year, with
356 summertime peaks due to OA compensated by wintertime enhancements in ammonium nitrate
357 and sea salt.

358 Figure 3 also shows an estimate of the aerosol all-sky DRF in 2100 from a GC-RT simulation
359 based on the RCP 4.5 emissions scenario. Due to the steep decline in SO_2 emissions (Table 1),
360 the global mean sulfate DRF drops by ~85% from 2010 to -0.031 Wm^{-2} . As shown by Pinder et
361 al. (2007), reductions in sulfate can lead to enhanced ammonium nitrate formation in
362 environments with abundant ammonia supply. Given that ammonia emissions in 2100 are
363 predicted to be approximately equivalent to those in 2010 in the RCP4.5 scenario, nitrate DRF in
364 2100 increases by 60% to -0.088 Wm^{-2} . Overall forcing from ammonium decreases (the decline
365 in ammonium sulfate outweighing the increase in ammonium nitrate) to -0.046 Wm^{-2} . Finally,
366 changes in BC and POA are more modest, but the magnitude of DRF decreases for both (to
367 0.056 and -0.053 Wm^{-2} respectively). Dust forcing is maintained at 2010 values. Overall the
368 clear-sky TOA DRF in 2100 (-0.22 Wm^{-2}) dropped by 39% from 2010. Smith and Bond (2013)

369 also estimate a precipitous decline (62%) in aerosol (carbonaceous and sulfate only) radiative
370 forcing from 2000 to 2100 when including both the direct and indirect forcing.

371

372 **4 Discussion and Conclusions**

373 We use the newly online coupled GEOS-Chem-RRTMG (GC-RT) global model to estimate
374 the direct radiative effect and directradiative forcing of atmospheric aerosols. The global TOA
375 DRE is over five times the cooling estimated as the DRF. This illustrates that tropospheric
376 aerosols exert a large influence on the global energy balance. However, the quantification of
377 DRE and DRF is highly uncertain and the estimate of the ratio between them is specific to this
378 model configuration and the concurrent assumptions. While the aerosol burden in the GEOS-
379 Chem model is well-tested against observations (e.g. (Zhang et al., 2012;Fisher et al.,
380 2011;Ridley et al., 2012;Jaegle et al., 2010;Lapina et al., 2011)), the uncertainties associated with
381 aerosol properties and radiative effects require further investigation.

382 Uncertainty in our estimates of DRF is dominated by the uncertainty in the MEE (as shown
383 by the AeroCom II study of Myhre et al. (2013)). Assumptions regarding size, water uptake and
384 absorption efficiency (e.g. the prevalence of brown carbon (Andreae and Gelencser, 2006)) all
385 contribute to this. We do not treat absorption enhancement from the coating of BC (Jacobson,
386 2000), the importance of which is unclear (Cappa et al., 2012;Lack et al., 2012), therefore both
387 DRE and DRF values may underestimate absorption. In addition to the uncertainty associated
388 with aerosol optics, our simulations likely underestimate the “anthropogenically-controlled”
389 SOA in the atmosphere, which is estimated to contribute -0.26 Wm^{-2} (Spracklen et al., 2011) of
390 direct cooling. The global source of dust arising from anthropogenic activity is also poorly
391 constrained.

392 Uncertainties in our estimate of DRE are likely even larger than uncertainties on DRF. This
393 is the result of: (1) better constraints on anthropogenic sectoral emissions (eg. mobile sources,
394 power generation) , (2) a poor understanding of natural particle emissions from ecosystems, both
395 marine and terrestrial (eg. terrestrial primary biological aerosol particles (e.g. (Heald and
396 Spracklen, 2009))), marine OA and methane sulfonate (Heintzenberg et al., 2000) – none of
397 which are included in this GC-RT simulation) and (3) the geographical extent and remoteness of
398 regions impacted by natural aerosols and hence a lack of measurement constraint (and thus well-
399 tested models).

400 We use Figure 6 to distinguish the definition of DRF and DRE of aerosols. The DRF is
401 linked to human-driven activities and neglects all feedbacks. The DRF accounts for the long-
402 term direct drivers of the climate system, which are primarily anthropogenic. In the case of
403 aerosols, this includes not only emission of primary particles (e.g. soot) and secondary aerosol
404 precursors (e.g. SO₂), but also the changes to the chemistry that governs the formation of
405 secondary aerosols. To the extent that this highly uncertain chemistry (including peroxy radical
406 chemistry and particle acidity) is included in models, it also contributes to the DRF (and its
407 uncertainty). This complicates the separation and interpretation of “anthropogenic” and “natural”
408 aerosol forcing. Anthropogenic land use change is also a driver of aerosol DRF (for example via
409 changes in dust, soil/vegetation, and ammonia emissions associated with crop expansion),
410 although it is rarely included in DRF assessments.

411 Figure 6a also illustrates the potential difference between an activity-based approach and an
412 agent-based approach to estimating RF. When associating a forcing with an agent, in this case
413 aerosols, all the radiative impacts described in Figure 6a are ascribed to this agent. This mirrors
414 the approach taken in previous IPCC reports (e.g. (IPCC, 2007, 2001)). Alternatively, an
415 activity-based approach, as suggested by Shindell et al. (2009) and used in the most recent IPCC
416 report (IPCC, 2013) can attribute the forcing with (controllable) behaviors such as emissions or
417 land use change.

418 Clearly, the DRF provides an incomplete estimate of the global radiative imbalance imposed
419 by changing aerosol abundance. Indeed, as anthropogenic emissions of aerosols and their
420 precursors are expected to continue to decline globally (van Vuuren et al., 2011), the aerosol
421 DRF will continue to decrease as shown here and by Smith and Bond (2013), diminishing its
422 relevance as a climate metric. At the same time feedbacks from climate change on aerosol are
423 likely to grow. This possibility was highlighted in the IPCC (2013): “climate change may alter
424 natural aerosol sources as well as removal by precipitation”. It is therefore critical that we
425 expand our set of metrics to address the many factors that the DRF neglects by design. Figure 6b
426 shows a more comprehensive set of drivers for changing aerosol abundance, including climate
427 feedbacks and natural emissions. In addition to the direct effect of aerosols on climate (the focus
428 of this study), the indirect effects of aerosols, both the conventional aerosol-cloud interactions
429 and the less-well constrained effect of aerosols on biogeochemistry (Mahowald, 2011), can
430 feedback on aerosol abundance via climate impacts. The relative importance of these feedbacks

431 and forcings on the global radiative flux imbalance over time is unclear and deserves further
432 investigation. The challenge of attributing a feedback is also non-trivial (e.g. to what agent does
433 one associate a temperature-driven change in aerosol abundance?). Inherently, the calculation of
434 DRE over time (with varying climate) includes the potential to quantify (though not attribute)
435 these effects. Furthermore, estimates of the aerosol indirect effect are very sensitive to the pre-
436 industrial aerosol burden, as originally shown by Menon et al. (2002) and more recently
437 discussed by Carslaw et al. (2013), for which little observational constraint exists. Thus, two
438 climate models with identical aerosol DRFs could provide very different estimates of the aerosol
439 indirect aerosol forcing due to differences in the pre-industrial (natural) aerosol burden.
440 Comparing the pre-industrial DRE simulated in models would provide a first step towards
441 identifying these key differences.

442 Quantifying and reporting the instantaneous DRE in global models is a simple and necessary
443 first step in going beyond the DRF metric for aerosols. While it may not directly serve as a
444 policy tool, the DRE is more easily tested against observations (e.g. satellites), is a more
445 thorough gauge for model comparisons, and offers a more complete picture of aerosols in the
446 climate system. As such, it is an important complement to the DRF for advancing our
447 understanding and predictions of the global aerosol burden and how it may counteract future
448 trends in greenhouse gas warming.

449

450 **Acknowledgements**

451 This work was supported by the EPA-STAR program and the Charles E. Reed Faculty Initiative
452 Fund. Although the research described in this article has been funded in part by the US EPA
453 through grant/cooperative agreement (RD-83503301), it has not been subjected to the Agency's
454 required peer and policy review and therefore does not necessarily reflect the views of the
455 Agency and no official endorsement should be inferred.

456 **References**

- 457 Alexander, B., Park, R. J., Jacob, D. J., Li, Q. B., Yantosca, R. M., Savarino, J., Lee, C. C. W.,
458 and Thiemens, M. H.: Sulfate formation in sea-salt aerosols: Constraints from oxygen isotopes, J.
459 Geophys. Res.-Atmos., 110, doi:10.1029/2004JD005659, D10307
460 Artn d10307, 2005.
- 461 Alvarado, M. J., Payne, V. H., Mlawer, E. J., Uymin, G., Shephard, M. W., Cady-Pereira, K. E.,
462 Delamere, J. S., and Moncet, J. L.: Performance of the Line-By-Line Radiative Transfer Model
463 (LBLRTM) for temperature, water vapor, and trace gas retrievals: recent updates evaluated with
464 IASI case studies, Atmos. Chem. Phys., 13, 6687-6711, doi:10.5194/acp-13-6687-2013, 2013.
- 465 Andreae, M. O., and Gelencser, A.: Black carbon or brown carbon? The nature of light-
466 absorbing carbonaceous aerosols, Atmospheric Chemistry and Physics, 6, 3131-3148, 2006.
- 467 Artaxo, P., Rizzo, L. V., Paixao, M., de Lucca, S., Oliveira, P. H., Lara, L. L., Wiedemann, K.
468 T., Andreae, M. O., Holben, B., Schafer, J., Correia, A. L., and Pauliquevis, T. M.: Aerosol
469 Particles in Amazonia: Their Composition, Role in the Radiation Balance, Cloud Formation, and
470 Nutrient Cycles, in: Amazonia and Global Change, Geophysical Monograph Series, 233-250,
471 2009.
- 472 Athanasopoulou, E., Vogel, H., Vogel, B., Tsimpidi, A. P., Pandis, S. N., Knote, C., and
473 Fountoukis, C.: Modeling the meteorological and chemical effects of secondary organic aerosols
474 during an EUCAARI campaign, Atmospheric Chemistry and Physics, 13, 625-645, 10.5194/acp-
475 13-625-2013, 2013.
- 476 Barker, H. W., Cole, J. N. S., Morcrette, J. J., Pincus, R., Raisanen, P., von Salzen, K., and
477 Vaillancourt, P. A.: The Monte Carlo Independent Column Approximation: An assessment using
478 several global atmospheric models, Q. J. R. Meteorol. Soc., 134, 1463-1478, 10.1002/qj.303,
479 2008.

480 Bellouin, N., Boucher, O., Haywood, J., and Reddy, M. S.: Global estimate of aerosol direct
481 radiative forcing from satellite measurements, *Nature*, 438, 1138-1141, 10.1038/nature04348,
482 2005.

483 Bellouin, N., Quaas, J., Morcrette, J. J., and Boucher, O.: Estimates of aerosol radiative forcing
484 from the MACC re-analysis, *Atmospheric Chemistry and Physics*, 13, 2045-2062, 10.5194/acp-
485 13-2045-2013, 2013.

486 Bond, T. C., and Bergstrom, R. W.: Light absorption by carbonaceous particles: An investigative
487 review, *Aerosol Science and Technology*, 40, 27-67, 10.1080/02786820500421521, 2006.

488 Bond, T. C., Bhardwaj, E., Dong, R., Jogani, R., Jung, S. K., Roden, C., Streets, D. G., and
489 Trautmann, N. M.: Historical emissions of black and organic carbon aerosol from energy-related
490 combustion, 1850-2000, *Glob. Biogeochem. Cycle*, 21, 16, Gb2018
491 10.1029/2006gb002840, 2007.

492 Bosilovich, M. G., Robertson, F. R., and Chen, J. Y.: Global Energy and Water Budgets in
493 MERRA, *Journal of Climate*, 24, 5721-5739, 10.1175/2011jcli4175.1, 2011.

494 Boucher, O., and Tanre, D.: Estimation of the aerosol perturbation to the Earth's radiative budget
495 over oceans using POLDER satellite aerosol retrievals, *Geophys. Res. Lett.*, 27, 1103-1106,
496 10.1029/1999gl010963, 2000.

497 Bouwman, A. F., Lee, D. S., Asman, W. A. H., Dentener, F. J., VanderHoek, K. W., and Olivier,
498 J. G. J.: A global high-resolution emission inventory for ammonia, *Glob. Biogeochem. Cycle*,
499 11, 561-587, 1997.

500 Cappa, C. D., Onasch, T. B., Massoli, P., Worsnop, D. R., Bates, T. S., Cross, E. S., Davidovits,
501 P., Hakala, J., Hayden, K. L., Jobson, B. T., Kolesar, K. R., Lack, D. A., Lerner, B. M., Li, S.
502 M., Mellon, D., Nuaaman, I., Olfert, J. S., Petaja, T., Quinn, P. K., Song, C., Subramanian, R.,

503 Williams, E. J., and Zaveri, R. A.: Radiative Absorption Enhancements Due to the Mixing State
504 of Atmospheric Black Carbon, *Science*, 337, 1078-1081, 10.1126/science.1223447, 2012.

505 Carslaw, K. S., Boucher, O., Spracklen, D. V., Mann, G. W., Rae, J. G. L., Woodward, S., and
506 Kulmala, M.: A review of natural aerosol interactions and feedbacks within the Earth system,
507 *Atmospheric Chemistry and Physics*, 10, 1701-1737, 2010.

508 Carslaw, K. S., Lee, L. A., Reddington, C. L., Pringle, K. J., Rap, A., Forster, P. M., Mann, G.
509 W., Spracklen, D. V., Woodhouse, M. T., Regayre, L. A., and Pierce, J. R.: Large contribution of
510 natural aerosols to uncertainty in indirect forcing, *Nature*, 503, 67-+, 10.1038/nature12674, 2013.

511 Chung, S. H., and Seinfeld, J. H.: Global distribution and climate forcing of carbonaceous
512 aerosols, *J. Geophys. Res.-Atmos.*, 107, doi:10.1029/2001JD001397, 4407
513 Artn 4407, 2002.

514 Clough, S. A., Iacono, M. J., and Moncet, J. L.: LINE-BY-LINE CALCULATIONS OF
515 ATMOSPHERIC FLUXES AND COOLING RATES - APPLICATION TO WATER-VAPOR,
516 *J. Geophys. Res.-Atmos.*, 97, 15761-15785, 1992.

517 Clough, S. A., Shephard, M. W., Mlawer, E., Delamere, J. S., Iacono, M., Cady-Pereira, K.,
518 Boukabara, S., and Brown, P. D.: Atmospheric radiative transfer modeling: a summary of the
519 AER codes, *J. Quant. Spectrosc. Radiat. Transf.*, 91, 233-244, 10.1016/j.jqsrt.2004.05.058, 2005.

520 Dentener, F., Kinne, S., Bond, T., Boucher, O., Cofala, J., Generoso, S., Ginoux, P., Gong, S.,
521 Hoelzemann, J. J., Ito, A., Marelli, L., Penner, J. E., Putaud, J. P., Textor, C., Schulz, M., van der
522 Werf, G. R., and Wilson, J.: Emissions of primary aerosol and precursor gases in the years 2000
523 and 1750 prescribed data-sets for AeroCom, *Atmospheric Chemistry and Physics*, 6, 4321-4344,
524 2006.

525 Drury, E. E., Jacob, D. J., Spurr, R. J. D., Wang, J., Shinozuka, Y., Anderson, B. E., Clarke, A.
526 D., Dibb, J., McNaughton, C., and Weber, R. J.: Synthesis of satellite (MODIS), aircraft
527 (ICARTT), and surface (IMPROVE, EPA-AQS, AERONET) aerosol observations over eastern
528 North America to improve MODIS aerosol retrievals and constrain aerosol concentrations and
529 sources, *J. Geophys. Res.-Atmos.*, 115, 2010.

530 Fairlie, T. D., Jacob, D. J., and Park, R. J.: The impact of transpacific transport of mineral dust in
531 the United States, *Atmospheric Environment*, 41, 1251-1266, 2007.

532 Fisher, J. A., Jacob, D. J., Wang, Q., Bahreini, R., Carouge, C. C., Cubison, M. J., Dibb, J. E.,
533 Diehl, T., Jimenez, J. L., Leibensperger, E. M., Meinders, M. B. J., Pye, H. O. T., Quinn, P. K.,
534 Sharma, S., van Donkelaar, A., and Yantosca, R. M.: Sources, distribution, and acidity of sulfate-
535 ammonium aerosol in the Arctic in winter-spring, *Atmos. Environ.*, 45, 7301-7318, 2011.

536 Ford, B., and Heald, C. L.: An A-train and model perspective on the vertical distribution of
537 aerosols and CO in the Northern Hemisphere, *J. Geophys. Res.-Atmos.*, 117,
538 doi:10.1029/2011JD016977, 2012.

539 Fountoukis, C., and Nenes, A.: ISORROPIA II: a computationally efficient thermodynamic
540 equilibrium model for K^+ - Ca^{2+} - Mg^{2+} - NH_4^+ - Na^+ - SO_4^{2-} - NO_3^- - Cl^- - H_2O aerosols,
541 *Atmospheric Chemistry and Physics*, 7, 4639-4659, 2007.

542 Fu, Q.: An accurate parameterization of the solar radiative properties of cirrus clouds for climate
543 models, *J. Climate.*, 9, 2058-2082, doi: [http://dx.doi.org/10.1175/1520-
544 0442\(1996\)009<2058:AAPOTS>2.0.CO;2](http://dx.doi.org/10.1175/1520-0442(1996)009<2058:AAPOTS>2.0.CO;2) 1996.

545 Fu, Q., Yang, P., and Sun, W. B.: An accurate parameterization of the infrared radiative
546 properties of cirrus clouds for climate models, *J. Climate.*, 11, 2223-2237, doi:
547 [http://dx.doi.org/10.1175/1520-0442\(1998\)011<2223:AAPOTI>2.0.CO;2](http://dx.doi.org/10.1175/1520-0442(1998)011<2223:AAPOTI>2.0.CO;2) 1998.

548 Ginoux, P., Prospero, J. M., Torres, O., and Chin, M.: Long-term simulation of global dust
549 distribution with the GOCART model: correlation with North Atlantic Oscillation,
550 *Environmental Modelling & Software*, 19, 113-128, 2004.

551 Goto, D., Takemura, T., and Nakajima, T.: Importance of global aerosol modeling including
552 secondary organic aerosol formed from monoterpene, *J. Geophys. Res.-Atmos.*, 113, 12, D07205
553 10.1029/2007jd009019, 2008.

554 Guenther, A., Karl, T., Harley, P., Wiedinmyer, C., Palmer, P. I., and Geron, C.: Estimates of
555 global terrestrial isoprene emissions using MEGAN (Model of Emissions of Gases and Aerosols
556 from Nature), *Atmospheric Chemistry and Physics*, 6, 3181-3210, 2006.

557 Heald, C. L., Jacob, D. J., Park, R. J., Russell, L. M., Huebert, B. J., Seinfeld, J. H., Liao, H., and
558 Weber, R. J.: A large organic aerosol source in the free troposphere missing from current
559 models, *Geophys. Res. Lett.*, 32, L18809,doi:10.1029/2005GL023831, 2005.

560 Heald, C. L., Henze, D. K., Horowitz, L. W., Feddema, J., Lamarque, J. F., Guenther, A., Hess,
561 P. G., Vitt, F., Seinfeld, J. H., Goldstein, A. H., and Fung, I.: Predicted change in global
562 secondary organic aerosol concentrations in response to future climate, emissions, and land use
563 change, *J. Geophys. Res.-Atmos.*, 113, D05211
564 Artn d05211, 2008.

565 Heald, C. L., and Spracklen, D. V.: Global budget of organic aerosol from fungal spores,
566 *Geophys. Res. Lett.*, 36, 2009.

567 Heald, C. L., Wilkinson, M. J., Monson, R. K., Alo, C. A., Wang, G. L., and Guenther, A.:
568 Response of isoprene emission to ambient CO₂ changes and implications for global budgets,
569 *Global Change Biology*, 15, 1127-1140, 10.1111/j.1365-2486.2008.01802.x, 2009.

570 Heald, C. L., Coe, H., Jimenez, J. L., Weber, R. J., Bahreini, R., Middlebrook, A. M., Russell, L.
571 M., Jolleys, M., Fu, T. M., Allan, J. D., Bower, K. N., Capes, G., Crosier, J., Morgan, W. T.,
572 Robinson, N. H., Williams, P. I., Cubison, J. J., DeCarlo, P. F., and Dunlea, E. J.: Exploring the
573 vertical profile of atmospheric organic aerosol: Comparing 17 aircraft field campaigns with a
574 global model, *Atmospheric Chemistry and Physics*, 11, 12673-12696, 2011.

575 Heald, C. L., Collett, J. L., Lee, T., Benedict, K. B., Schwandner, F. M., Li, Y., Clarisse, L.,
576 Hurtmans, D. R., Van Damme, M., Clerbaux, C., Coheur, P. F., Philip, S., Martin, R. V., and
577 Pye, H. O. T.: Atmospheric ammonia and particulate inorganic nitrogen over the United States,
578 *Atmospheric Chemistry and Physics*, 12, 10295-10312, 10.5194/acp-12-10295-2012, 2012.

579 Heintzenberg, J., Covert, D. C., and Van Dingenen, R.: Size distribution and chemical
580 composition of marine aerosols: a compilation and review, *Tellus Ser. B-Chem. Phys. Meteorol.*,
581 52, 1104-1122, 10.1034/j.1600-0889.2000.00136.x, 2000.

582 Henze, D. K., and Seinfeld, J. H.: Global secondary organic aerosol from isoprene oxidation,
583 *Geophys. Res. Lett.*, 33, doi:10.1029/2006GL025976, L09812
584 Artn 109812, 2006.

585 Henze, D. K., Seinfeld, J. H., Ng, N. L., Kroll, J. H., Fu, T. M., Jacob, D. J., and Heald, C. L.:
586 Global modeling of secondary organic aerosol formation from aromatic hydrocarbons: high- vs.
587 low-yield pathways, *Atmospheric Chemistry and Physics*, 8, 2405-2420, 2008.

588 Hess, M., Koepke, P., and Schult, I.: Optical properties of aerosols and clouds: The software
589 package OPAC, *Bull. Amer. Meteorol. Soc.*, 79, 831-844, 1998.

590 Holmes, C. D., Prather, M. J., Sovde, O. A., and Myhre, G.: Future methane, hydroxyl, and their
591 uncertainties: key climate and emission parameters for future predictions, *Atmospheric*
592 *Chemistry and Physics*, 13, 285-302, 10.5194/acp-13-285-2013, 2013.

593 Hu, Y. X., and Stamnes, K.: An Accurate Parameterization of the Radiative Properties of Water
594 Clouds Suitable for Use in Climate Models *J. Climate.*, 6, 728-742, doi:
595 [http://dx.doi.org/10.1175/1520-0442\(1993\)006<0728:AAPOTR>2.0.CO;2](http://dx.doi.org/10.1175/1520-0442(1993)006<0728:AAPOTR>2.0.CO;2) 1993.

596 Iacono, M. J., Delamere, J. S., Mlawer, E. J., and Clough, S. A.: Evaluation of upper
597 tropospheric water vapor in the NCAR Community Climate Model (CCM3) using modeled and
598 observed HIRS radiances, *J. Geophys. Res.-Atmos.*, 108, 4037
599 10.1029/2002jd002539, 2003.

600 Iacono, M. J., Delamere, J. S., Mlawer, E. J., Shephard, M. W., Clough, S. A., and Collins, W.
601 D.: Radiative forcing by long-lived greenhouse gases: Calculations with the AER radiative
602 transfer models, *J. Geophys. Res.-Atmos.*, 113, D13103
603 10.1029/2008jd009944, 2008.

604 IPCC: *Climate Change: The IPCC Scientific Assessment*, Cambridge, UK, 365 pp., 1990.
605 IPCC: *Climate Change 1995: The Science of Climate Change*, Cambridge, UK, 573 pp., 1995.
606 IPCC: *Climate Change 2001: The Scientific Basis*, edited by: Houghton, J. T. e. a., Cambridge
607 University Press, Cambridge, UK, 881 pp., 2001.

608 IPCC: *Climate Change 2007: The Physical Science Basis*, edited by: Solomon, S. e. a.,
609 Cambridge University Press, Cambridge, UK, 996 pp., 2007.

610 IPCC: *Climate Change 2013: The Physical Science Basis: Summary for Policymakers*,
611 Cambridge, UK, 2013.

612 Jacobson, M. Z.: A physically-based treatment of elemental carbon optics: Implications for
613 global direct forcing of aerosols, *Geophys. Res. Lett.*, 27, 217-220, 2000.

614 Jaegle, L., Quinn, P. K., Bates, T. S., Alexander, B., and Lin, J.-T.: Global distribution of sea salt
615 aerosols: new constraints from in situ and remote sensing observations, *Atmos. Chem. Phys.*
616 *Discuss.*, 10, 25687-25742, 2010.

617 Jo, D. S., Park, R. J., Kim, M. J., and Spracklen, D. V.: Effects of chemical aging on global
618 secondary organic aerosol using the volatility basis set approach, *Atmos. Environ.*,
619 <http://dx.doi.org/10.1016/j.atmosenv.2013.08.055>, 2013.

620 Kim, J., Yoon, S. C., Kim, S. W., Brechtel, F., Jefferson, A., Dutton, E. G., Bower, K. N., Cliff,
621 S., and Schauer, J. J.: Chemical apportionment of shortwave direct aerosol radiative forcing at
622 the Gosan super-site, Korea during ACE-Asia, *Atmos. Environ.*, 40, 6718-6729,
623 [10.1016/j.atmosenv.2006.06.007](http://dx.doi.org/10.1016/j.atmosenv.2006.06.007), 2006.

624 Kinne, S., Schulz, M., Textor, C., Guibert, S., Balkanski, Y., Bauer, S. E., Berntsen, T., Berglen,
625 T. F., Boucher, O., Chin, M., Collins, W., Dentener, F., Diehl, T., Easter, R., Feichter, J.,
626 Fillmore, D., Ghan, S., Ginoux, P., Gong, S., Grini, A., Hendricks, J. E., Herzog, M., Horowitz,
627 L., Isaksen, I., Iversen, T., Kirkavag, A., Kloster, S., Koch, D., Kristjansson, J. E., Krol, M.,
628 Lauer, A., Lamarque, J. F., Lesins, G., Liu, X., Lohmann, U., Montanaro, V., Myhre, G., Penner,
629 J. E., Pitari, G., Reddy, S., Seland, O., Stier, P., Takemura, T., and Tie, X.: An AeroCom initial
630 assessment - optical properties in aerosol component modules of global models, *Atmospheric*
631 *Chemistry and Physics*, 6, 1815-1834, 2006.

632 Koch, D., Schulz, M., Kinne, S., McNaughton, C., Spackman, J. R., Balkanski, Y., Bauer, S.,
633 Berntsen, T., Bond, T. C., Boucher, O., Chin, M., Clarke, A., De Luca, N., Dentener, F., Diehl,
634 T., Dubovik, O., Easter, R., Fahey, D. W., Feichter, J., Fillmore, D., Freitag, S., Ghan, S.,
635 Ginoux, P., Gong, S., Horowitz, L., Iversen, T., Kirkevag, A., Klimont, Z., Kondo, Y., Krol, M.,
636 Liu, X., Miller, R., Montanaro, V., Moteki, N., Myhre, G., Penner, J. E., Perlwitz, J., Pitari, G.,

637 Reddy, S., Sahu, L., Sakamoto, H., Schuster, G., Schwarz, J. P., Seland, O., Stier, P., Takegawa,
638 N., Takemura, T., Textor, C., van Aardenne, J. A., and Zhao, Y.: Evaluation of black carbon
639 estimations in global aerosol models, *Atmospheric Chemistry and Physics*, 9, 9001-9026, 2009.

640 Kopke, P., Hess, M., Schult, I., and Shettle, E. P.: Global aerosol data set, Max Planck Inst. fur
641 Meteorol., Hamburg, Germany, 1997.

642 Lacis, A. A., and Oinas, V.: A description of the correlated kappa-distribution method for
643 modeling nongray gaseous absorption, thermal emission, and multiple-scattering in vertically
644 inhomogeneous atmosphere *J. Geophys. Res.-Atmos.*, 96, 9027-9063, 10.1029/90jd01945, 1991.

645 Lack, D. A., Langridge, J. M., Bahreini, R., Cappa, C. D., Middlebrook, A. M., and Schwarz, J.
646 P.: Brown carbon and internal mixing in biomass burning particles, *Proc. Natl. Acad. Sci. U. S.*
647 *A.*, 109, 14802-14807, 10.1073/pnas.1206575109, 2012.

648 Lapina, K., Heald, C. L., Spracklen, D. V., Arnold, S. R., Bates, T. S., Allan, J. D., Coe, H.,
649 McFiggans, G., Zorn, S. R., Drewnick, F., Hind, A., and Smirnov, A.: Investigating organic
650 aerosol loading in the remote marine environment, *Atmos. Chem. Phys.*, 11, 8847–8860,
651 doi:10.5194/acp-11-8847-2011, 2011.

652 Liao, H., Seinfeld, J. H., Adams, P. J., and Mickley, L. J.: Global radiative forcing of coupled
653 tropospheric ozone and aerosols in a unified general circulation model, *J. Geophys. Res.-Atmos.*,
654 109, D16207
655 10.1029/2003jd004456, 2004.

656 Liu, H. Y., Jacob, D. J., Bey, I., and Yantosca, R. M.: Constraints from Pb-210 and Be-7 on wet
657 deposition and transport in a global three-dimensional chemical tracer model driven by
658 assimilated meteorological fields, *J. Geophys. Res.-Atmos.*, 106, 12109-12128, 2001.

659 Ma, X., Yu, F., and Luo, G.: Aerosol direct radiative forcing based on GEOS-Chem-APM and
660 uncertainties, *Atmospheric Chemistry and Physics*, 12, 5563-5581, 10.5194/acp-12-5563-2012,
661 2012.

662 Mahowald, N.: Aerosol Indirect Effect on Biogeochemical Cycles and Climate, *Science*, 334,
663 794-796, 10.1126/science.1207374, 2011.

664 Mahowald, N. M., and Luo, C.: A less dusty future?, *Geophys. Res. Lett.*, 30, 4, 1903
665 10.1029/2003gl017880, 2003.

666 Mahowald, N. M., Yoshioka, M., Collins, W. D., Conley, A. J., Fillmore, D. W., and Coleman,
667 D. B.: Climate response and radiative forcing from mineral aerosols during the last glacial
668 maximum, pre-industrial, current and doubled-carbon dioxide climates, *Geophys. Res. Lett.*, 33,
669 4, L20705
670 10.1029/2006gl026126, 2006.

671 Massoli, P., Bates, T. S., Quinn, P. K., Lack, D. A., Baynard, T., Lerner, B. M., Tucker, S. C.,
672 Brioude, J., Stohl, A., and Williams, E. J.: Aerosol optical and hygroscopic properties during
673 TexAQS-GoMACCS 2006 and their impact on aerosol direct radiative forcing, *J. Geophys. Res.-*
674 *Atmos.*, 114, D00f07
675 10.1029/2008jd011604, 2009.

676 Menon, S., Del Genio, A. D., Koch, D., and Tselioudis, G.: GCM Simulations of the aerosol
677 indirect effect: Sensitivity to cloud parameterization and aerosol burden, *J. Atmos. Sci.*, 59, 692-
678 713, 10.1175/1520-0469(2002)059<0692:gsotai>2.0.co;2, 2002.

679 Mlawer, E. J., Taubman, S. J., Brown, P. D., Iacono, M. J., and Clough, S. A.: Radiative transfer
680 for inhomogeneous atmospheres: RRTM, a validated correlated-k model for the longwave, *J.*
681 *Geophys. Res.-Atmos.*, 102, 16663-16682, 10.1029/97jd00237, 1997.

682 Mlawer, E. J., and Clough, S. A.: Shortwave and longwave enhancements in the rapid radiative
683 transfer model, 7th Atmospheric Radiation Measurement (ARM) Science Team Meeting, San
684 Antonia, Texas, 1998, 409-413,

685 Myhre, G., Samset, B. H., Schulz, M., Balkanski, Y., Bauer, S., Berntsen, T. K., Bian, H.,
686 Bellouin, N., Chin, M., Diehl, T., Easter, R. C., Feichter, J., Ghan, S. J., Hauglustaine, D.,
687 Iversen, T., Kinne, S., Kirkevag, A., Lamarque, J. F., Lin, G., Liu, X., Lund, M. T., Luo, G., Ma,
688 X., van Noije, T., Penner, J. E., Rasch, P. J., Ruiz, A., Seland, O., Skeie, R. B., Stier, P.,
689 Takemura, T., Tsigaridis, K., Wang, P., Wang, Z., Xu, L., Yu, H., Yu, F., Yoon, J. H., Zhang, K.,
690 Zhang, H., and Zhou, C.: Radiative forcing of the direct aerosol effect from AeroCom Phase II
691 simulations, *Atmospheric Chemistry and Physics*, 13, 1853-1877, 10.5194/acp-13-1853-2013,
692 2013.

693 Olivier, J. G. J., Berdowski, J. J. M., Peters, J. A. H. W., Bakker, J., Visschedijk, A. J. H., and J.-
694 P.J.Bloos: Applications of EDGAR Including a description of EDGAR 3.0: reference database
695 with trend data for 1970-1995 Natl. Inst. of Public Health and Environ., Bilthoven, Netherlands,
696 2001.

697 Oreopoulos, L., and Mlawer, E.: THE CONTINUAL INTERCOMPARISON OF RADIATION
698 CODES (CIRC) Assessing Anew the Quality of GCM Radiation Algorithms, *Bull. Amer.*
699 *Meteorol. Soc.*, 91, 305-310, 10.1175/2009bams2732.1, 2010.

700 Oreopoulos, L., Mlawer, E., Delamere, J., Shippert, T., Cole, J., Fomin, B., Iacono, M., Jin, Z.
701 H., Li, J. N., Manners, J., Raisanen, P., Rose, F., Zhang, Y. C., Wilson, M. J., and Rossow, W.
702 B.: The Continual Intercomparison of Radiation Codes: Results from Phase I, *J. Geophys. Res.-*
703 *Atmos.*, 117, 19, D06118
704 10.1029/2011jd016821, 2012.

705 Park, R. J., Jacob, D. J., Chin, M., and Martin, R. V.: Sources of carbonaceous aerosols over the
706 United States and implications for natural visibility, *J. Geophys. Res.-Atmos.*, 108,
707 doi:10.1029/2002JD003190, 4355
708 Artn 4355, 2003.

709 Park, R. J., Jacob, D. J., Field, B. D., Yantosca, R. M., and Chin, M.: Natural and transboundary
710 pollution influences on sulfate-nitrate-ammonium aerosols in the United States: Implications for
711 policy, *J. Geophys. Res.-Atmos.*, 109, D15204, doi:10.1029/2003JD004473, 2004.

712 Park, R. J., Jacob, D. J., Kumar, N., and Yantosca, R. M.: Regional visibility statistics in the
713 United States: Natural and transboundary pollution influences, and implications for the Regional
714 Haze Rule, *Atmos. Environ.*, 40, 5405-5423, 2006.

715 Pincus, R., Barker, H. W., and Morcrette, J. J.: A fast, flexible, approximate technique for
716 computing radiative transfer in inhomogeneous cloud fields, *J. Geophys. Res.-Atmos.*, 108, 5,
717 4376
718 10.1029/2002jd003322, 2003.

719 Pinder, R. W., Adams, P. J., and Pandis, S. N.: Ammonia emission controls as a cost-effective
720 strategy for reducing atmospheric particulate matter in the eastern United States, *Environ. Sci.*
721 *Technol.*, 41, 380-386, 10.1021/es060379a, 2007.

722 Pye, H. O. T., Liao, H., Wu, S., Mickley, L. J., Jacob, D. J., Henze, D. K., and Seinfeld, J. H.:
723 Effect of changes in climate and emissions on future sulfate-nitrate-ammonium aerosol levels in
724 the United States, *J. Geophys. Res.-Atmos.*, 114, 18, D01205
725 10.1029/2008jd010701, 2009.

726 Raes, F., Liao, H., Chen, W. T., and Seinfeld, J. H.: Atmospheric chemistry-climate feedbacks, *J.*
727 *Geophys. Res.-Atmos.*, 115, 14, D12121

728 10.1029/2009jd013300, 2010.

729 Rap, A., Scott, C. E., Spracklen, D. V., Bellouin, N., Forster, P. M., Carslaw, K. S., Schmidt, A.,
730 and Mann, G.: Natural aerosol direct and indirect radiative effects, *Geophys. Res. Lett.*, 40,
731 3297-3301, 10.1002/grl.50441, 2013.

732 Ridley, D. A., Heald, C. L., and Ford, B. J.: North African Dust Export and Impacts: An
733 Integrated Satellite and Model Perspective, *J. Geophys. Res.-Atmos.*, 117,
734 doi:10.1029/2011JD016794, 2012.

735 Ridley, D. A., Heald, C. L., and Prospero, J. M.: What controls the recent changes in African
736 mineral dust aerosol across the Atlantic?, *Atmos. Chem. Phys. Discuss.*, submitted.

737 Rothman, L. S., Jacquemart, D., Barbe, A., Benner, D. C., Birk, M., Brown, L. R., Carleer, M.
738 R., Chackerian, C., Chance, K., Coudert, L. H., Dana, V., Devi, V. M., Flaud, J. M., Gamache,
739 R. R., Goldman, A., Hartmann, J. M., Jucks, K. W., Maki, A. G., Mandin, J. Y., Massie, S. T.,
740 Orphal, J., Perrin, A., Rinsland, C. P., Smith, M. A. H., Tennyson, J., Tolchenov, R. N., Toth, R.
741 A., Vander Auwera, J., Varanasi, P., and Wagner, G.: The HITRAN 2004 molecular
742 spectroscopic database, *J. Quant. Spectrosc. Radiat. Transf.*, 96, 139-204,
743 10.1016/j.jqsrt.2004.10.008, 2005.

744 Schaaf, C. B., Gao, F., Strahler, A. H., Lucht, W., Li, X. W., Tsang, T., Strugnell, N. C., Zhang,
745 X. Y., Jin, Y. F., Muller, J. P., Lewis, P., Barnsley, M., Hobson, P., Disney, M., Roberts, G.,
746 Dunderdale, M., Doll, C., d'Entremont, R. P., Hu, B. X., Liang, S. L., Privette, J. L., and Roy, D.:
747 First operational BRDF, albedo nadir reflectance products from MODIS, *Remote Sens. Environ.*,
748 83, 135-148, 10.1016/s0034-4257(02)00091-3, 2002.

749 Schultz, M. G.: REanalysis of the TROpospheric chemical composition over the past 40 years
750 Max Planck Institute for Meteorology, Julich/Hamburg, Germany, 2007.

751 Schwarz, J. P., Spackman, J. R., Gao, R. S., Watts, L. A., Stier, P., Schulz, M., Davis, S. M.,
752 Wofsy, S. C., and Fahey, D. W.: Global-scale black carbon profiles observed in the remote
753 atmosphere and compared to models, *Geophys. Res. Lett.*, 37, 5, L18812
754 10.1029/2010gl044372, 2010.

755 Shindell, D. T., Faluvegi, G., Koch, D. M., Schmidt, G. A., Unger, N., and Bauer, S. E.:
756 Improved Attribution of Climate Forcing to Emissions, *Science*, 326, 716-718,
757 10.1126/science.1174760, 2009.

758 Shindell, D. T., Lamarque, J. F., Schulz, M., Flanner, M., Jiao, C., Chin, M., Young, P. J., Lee,
759 Y. H., Rotstajn, L., Mahowald, N., Milly, G., Faluvegi, G., Balkanski, Y., Collins, W. J.,
760 Conley, A. J., Dalsoren, S., Easter, R., Ghan, S., Horowitz, L., Liu, X., Myhre, G., Nagashima,
761 T., Naik, V., Rumbold, S. T., Skeie, R., Sudo, K., Szopa, S., Takemura, T., Voulgarakis, A.,
762 Yoon, J. H., and Lo, F.: Radiative forcing in the ACCMIP historical and future climate
763 simulations, *Atmospheric Chemistry and Physics*, 13, 2939-2974, 10.5194/acp-13-2939-2013,
764 2013.

765 Sidran, M.: Broad-Band Reflectance and Emissivity of Specular and Rough Water Surface,
766 *Applied Optics*, 20, 3176-3183, doi: 10.1364/AO.20.003176, 1981.

767 Sinyuk, A., Torres, O., and Dubovik, O.: Combined use of satellite and surface observations to
768 infer the imaginary part of refractive index of Saharan dust, *Geophys. Res. Lett.*, 30, 4, 1081
769 10.1029/2002gl016189, 2003.

770 Smith, S. J., and Bond, T. C.: Two hundred and fifty years of aerosols and climate: the end of the
771 age of aerosols, *Atmos. Chem. Phys. Discuss.*, 13, 6419-6453, doi:10.5194/acpd-13-6419-2013,
772 2013.

773 Spracklen, D. V., Mickley, L. J., Logan, J. A., Hudman, R. C., Yevich, R., Flannigan, M. D., and
774 Westerling, A. L.: Impacts of climate change from 2000 to 2050 on wildfire activity and
775 carbonaceous aerosol concentrations in the western United States, *J. Geophys. Res.-Atmos.*, 114,
776 17, D20301
777 10.1029/2008jd010966, 2009.

778 Spracklen, D. V., Jimenez, J. L., Carslaw, K. S., Worsnop, D. R., Evans, M. J., Mann, G. W.,
779 Zhang, Q., M.R., C., Allan, J., Coe, H., McFiggans, G., Rap, A., and Forster, P.: Aerosol mass
780 spectrometer constraint on the global secondary organic aerosol budget, *Atmos. Chem. Phys.* ,
781 11, 12109-12136, doi:10.5194/acp-11-12109-2011, 2011.

782 Stier, P., Seinfeld, J. H., Kinne, S., and Boucher, O.: Aerosol absorption and radiative forcing,
783 *Atmospheric Chemistry and Physics*, 7, 5237-5261, 2007.

784 Tegen, I., and Lacis, A. A.: Modeling of particle size distribution and its influence on the
785 radiative properties of mineral dust aerosol, *J. Geophys. Res.-Atmos.*, 101, 19237-19244, 1996.

786 Tegen, I., Werner, M., Harrison, S. P., and Kohfeld, K. E.: Relative importance of climate and
787 land use in determining present and future global soil dust emission, *Geophys. Res. Lett.*, 31, 4,
788 L05105
789 10.1029/2003gl019216, 2004.

790 Tsigaridis, K., and Kanakidou, M.: Secondary organic aerosol importance in the future
791 atmosphere, *Atmos. Environ.*, 41, 4682-4692, 2007.

792 van der Werf, G. R., Randerson, J. T., Giglio, L., Collatz, G. J., Mu, M., Kasibhatla, P. S.,
793 Morton, D. C., DeFries, R. S., Jin, Y., and van Leeuwen, T. T.: Global fire emissions and the
794 contribution of deforestation, savanna, forest, agricultural, and peat fires (1997-2009),
795 *Atmospheric Chemistry and Physics*, 10, 11707-11735, 10.5194/acp-10-11707-2010, 2010.

796 van Donkelaar, A., Martin, R. V., Leaitch, W. R., Macdonald, A. M., Walker, T. W., Streets, D.
797 G., Zhang, Q., Dunlea, E. J., Jimenez, J. L., Dibb, J. E., Huey, L. G., Weber, R., and Andreae, M.
798 O.: Analysis of aircraft and satellite measurements from the Intercontinental Chemical Transport
799 Experiment (INTEX-B) to quantify long-range transport of East Asian sulfur to Canada,
800 *Atmospheric Chemistry and Physics*, 8, 2999-3014, 2008.

801 van Vuuren, D. P., Edmonds, J., Kainuma, M., Riahi, K., Thomson, A., Hibbard, K., Hurtt, G.
802 C., Kram, T., Krey, V., Lamarque, J. F., Masui, T., Meinshausen, M., Nakicenovic, N., Smith, S.
803 J., and Rose, S. K.: The representative concentration pathways: an overview, *Clim. Change*, 109,
804 5-31, 10.1007/s10584-011-0148-z, 2011.

805 Wan, Z. M., Zhang, Y. L., Zhang, Q. C., and Li, Z. L.: Validation of the land-surface
806 temperature products retrieved from Terra Moderate Resolution Imaging Spectroradiometer data,
807 *Remote Sens. Environ.*, 83, 163-180, 10.1016/s0034-4257(02)00093-7, 2002.

808 Wang, Q., Jacob, D. J., Fisher, J. A., Mao, J., Leibensperger, E. M., Carouge, C. C., LeSager, P.,
809 Kondo, Y., Jimenez, J. L., Cubison, M. J., and Doherty, S. J.: Sources of carbonaceous aerosols
810 and deposited black carbon in the Arctic in winter-spring: implications for radiative forcing,
811 *Atmospheric Chemistry and Physics*, 11, 12453-12473, 2011.

812 Westerling, A. L., Hidalgo, H. G., Cayan, D. R., and Swetnam, T. W.: Warming and earlier
813 spring increase western US forest wildfire activity, *Science*, 313, 940-943,
814 10.1126/science.1128834, 2006.

815 Wild, O., Zhu, X., and Prather, M. J.: Fast-j: Accurate simulation of in- and below-cloud
816 photolysis in tropospheric chemical models, *J. Atmos. Chem.*, 37, 245-282,
817 10.1023/a:1006415919030, 2000.

818 Yevich, R., and Logan, J. A.: An assessment of biofuel use and burning of agricultural waste in
819 the developing world, *Glob. Biogeochem. Cycle*, 17, 10.1029/2002GB001952 2003.

820 Yu, H., Kaufman, Y. J., Chin, M., Feingold, G., Remer, L. A., Anderson, T. L., Balkanski, Y.,
821 Bellouin, N., Boucher, O., Christopher, S., DeCola, P., Kahn, R., Koch, D., Loeb, N., Reddy, M.
822 S., Schulz, M., Takemura, T., and Zhou, M.: A review of measurement-based assessments of the
823 aerosol direct radiative effect and forcing, *Atmospheric Chemistry and Physics*, 6, 613-666,
824 2006.

825 Zender, C. S., Bian, H. S., and Newman, D.: Mineral Dust Entrainment and Deposition (DEAD)
826 model: Description and 1990s dust climatology, *J. Geophys. Res.-Atmos.*, 108, 4416
827 Artn 4416, 2003.

828 Zhang, L., Jacob, D. J., Knipping, E. M., Kumar, N., Munger, J. W., Carouge, C. C., van
829 Donkelaar, A., Wang, Y. X., and Chen, D.: Nitrogen deposition to the United States: distribution,
830 sources and processes, *Atmospheric Chemistry and Physics*, 12, 4539-4554, 10.5194/acp-12-
831 4539-2012, 2012.

832 Zhang, L. M., Gong, S. L., Padro, J., and Barrie, L.: A size-segregated particle dry deposition
833 scheme for an atmospheric aerosol module, *Atmos. Environ.*, 35, 549-560, 2001.

834

835

Table 1. Annual global aerosol or aerosol precursor emissions for used in GC-RT

| | Total Emissions (2010) | Anthropogenic Emissions¹ and Percent of Total in Brackets (2010) | Total Emissions (2100) |
|--|-------------------------------|--|-------------------------------|
| SOx (TgSyr⁻¹) | 63.8 | 53.3 (83%) | 19.5 |
| NOx (TgNyr⁻¹) | 49.4 | 31.8 (64%) | 28.0 |
| NH₃ (TgNyr⁻¹) | 55.9 | 37.9 (68%) | 56.3 |
| POA (TgCyr⁻¹) | 29.3 | 9.3 (32%) | 20.4 |
| BC (TgCyr⁻¹) | 6.8 | 4.5 (66%) | 4.4 |
| Sea Salt (Tgyr⁻¹) | 3544 | - | 3544 |
| Dust (Tgyr⁻¹) | 1563 | 312 (20%) | 1563 |

Table 2. GC-RT speciated dry aerosol size and optical properties

| | Geometric radius (r_g) (μm) | Geometric Stdev (σ_g, log(μm)) | Refractive Index (550 nm) | Density (gcm⁻³) |
|--------------------------------------|--|---|----------------------------------|-----------------------------------|
| Sulfate, Nitrate and Ammonium | 0.070 | 1.6 | 1.53-0.006i | 1.7 |
| OA | 0.064 | 1.6 | 1.53-0.006i | 1.8 |
| BC | 0.020 | 1.6 | 1.95-0.79i | 1.8 |
| Sea Salt | | | | |
| accumulation | 0.085 | 1.5 | 1.50-0.00000001i | 2.2 |
| coarse | 0.40 | 1.8 | 1.50-0.00000001i | 2.2 |
| Dust | 7 bins: 0.015, 0.25, 0.40, 0.80, 1.5, 2.5, 4.0 | 2.2 | 1.56-0.0014i | 2.5 |

¹ Includes fossil fuel, biofuel, and agriculture (but not biomass burning)

Table 3. Global annual mean aerosol budget and impacts simulated for 2010 using GC-RT (comparisons with AEROCOM II means from Myhre et al., 2013 in round brackets; comparisons with AEROCOM I medians from Kinne et al. 2006 in square brackets). Note anthropogenic here does not include biomass burning.

| | Total | Sulfate | Nitrate | Ammonium ² | BC | OA ³ | Sea Salt | Dust |
|--|-------------------------------------|----------------------------|---------------------------|-----------------------|----------------------------|---------------------------|------------------|------------------|
| Burden [Tg] | | 1.27 [1.99] | 0.26 | 0.35 | 0.10 [0.20] | 2.01 [1.68] | 3.94 [6.43] | 22.9 [19.9] |
| Anthropogenic Fraction | | 0.60 | 0.82 | 0.82 | 0.57 | 0.21 | 0.0 | 0.20 |
| Anthropogenic Burden [Tg] | | 0.76 (0.91±0.24) | 0.21 (0.29±0.14) | 0.29 | 0.057 (0.071±0.036) | 0.44 (0.33±0.23) | 0.0 | 4.57 |
| AOD, 550 nm | 0.092 | 0.0154 [0.034] | 0.0031 | 0.0041 | 0.0012 [0.004] | 0.0147 [0.019] | 0.032 [0.030] | 0.021 [0.032] |
| Anthro AOD, 550 nm | 0.023 (0.030±0.01) | 0.0092 (0.021±0.009) | 0.0025 (0.0056±0.0027) | 0.0034 | 0.0007 (0.0015±0.0005) | 0.0029 (0.0062±0.0071) | 0.0 | 0.004 |
| MEE=AOD/burden [m² g⁻¹] | | 6.3 (12.7±8.6) [8.5] | 5.7 (9.8±2.0) | 5.9 | 5.9 (10.5±3.9) [8.9] | 3.8 (7.5±6.5) [5.7] | 4.1 [3.0] | 0.47 [0.95] |
| TOA DRE, clear-sky [Wm⁻²] | -2.75 | -0.54 | -0.095 | -0.14 | 0.10 | -0.61 | -1.10 | -0.37 |
| SW | -3.01 | -0.55 | -0.097 | -0.14 | 0.10 | -0.63 | -1.16 | -0.53 |
| LW | 0.26 | 0.01 | 0.002 | 0.003 | 0.002 | 0.02 | 0.06 | 0.16 |
| TOA DRE, all-sky [Wm⁻²] | -1.83 | -0.35 | -0.067 | -0.095 | 0.14 | -0.42 | -0.77 | -0.26 |
| SW | -2.03 | -0.36 | -0.069 | -0.097 | 0.14 | -0.43 | -0.81 | -0.40 |
| LW | 0.19 | 0.007 | 0.002 | 0.002 | 0.001 | 0.01 | 0.04 | 0.14 |
| TOA DRF, clear-sky [Wm⁻²] | -0.57 (-0.67±0.18) | -0.29 | -0.079 | -0.11 | 0.06 | -0.075 | 0.0 | -0.074 |
| TOA DRF, all-sky [Wm⁻²] | -0.36 (-0.32 ⁴ ±0.15) | -0.20 (-0.32±0.11) | -0.055 (-0.08±0.04) | -0.076 | 0.078 (0.18±0.07) | -0.055 (-0.09) | 0.0 | -0.053 |

² Contributions from ammonium are included in sulfate and nitrate in AeroCom II

³ we sum POA and SOA mean model values from AeroCom II

⁴ Taken from Figure 7 of Myhre et al., 2013

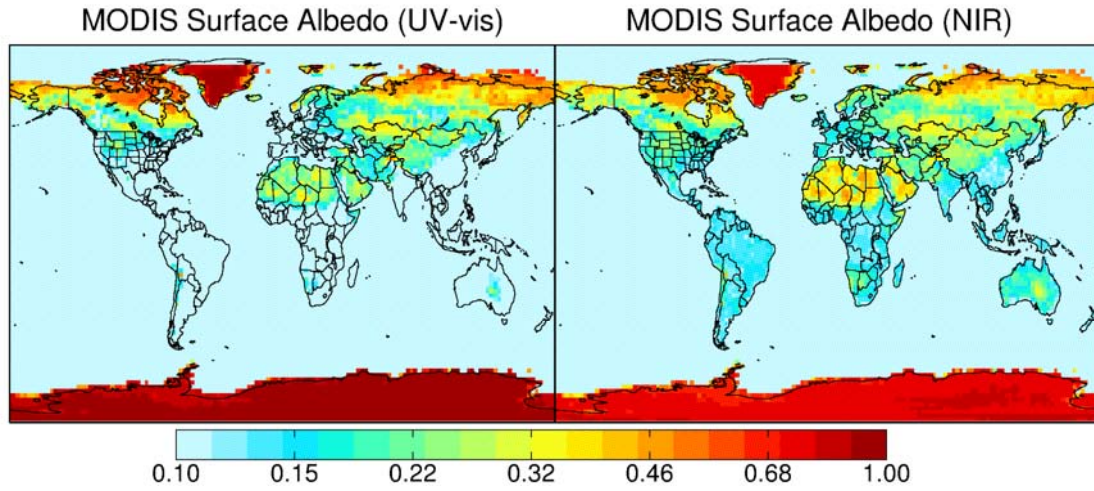


Figure 1. Annual mean surface direct albedo in the UV-visible (left) and near-infrared (right) from MODIS 2002-2007 observations.

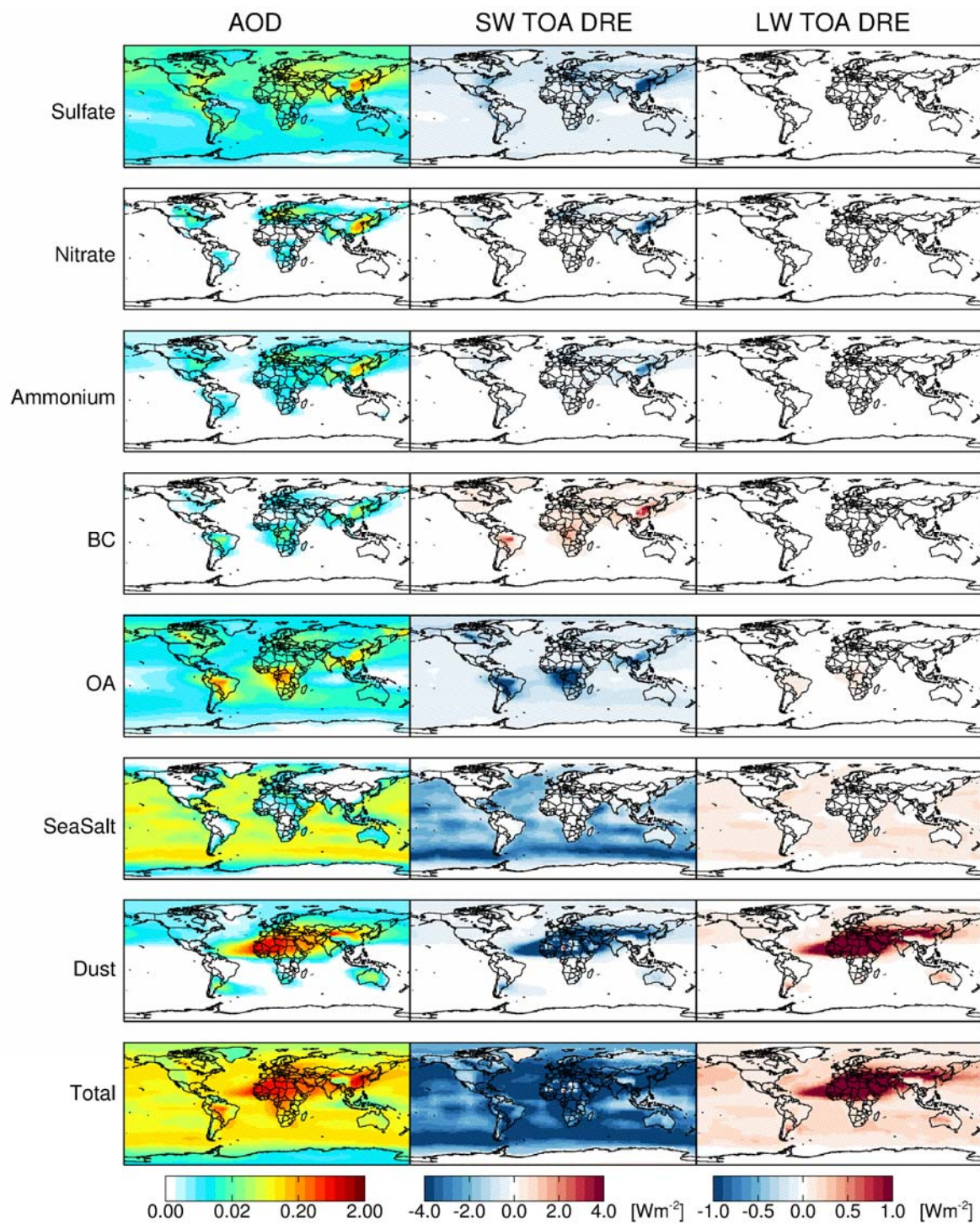


Figure 2. Annual mean AOD (left), shortwave TOA clear-sky direct radiative effect (center) and longwave TOA clear-sky direct radiative effect (right) simulated by GC-RT for 2010. Color bars are saturated at respective values.

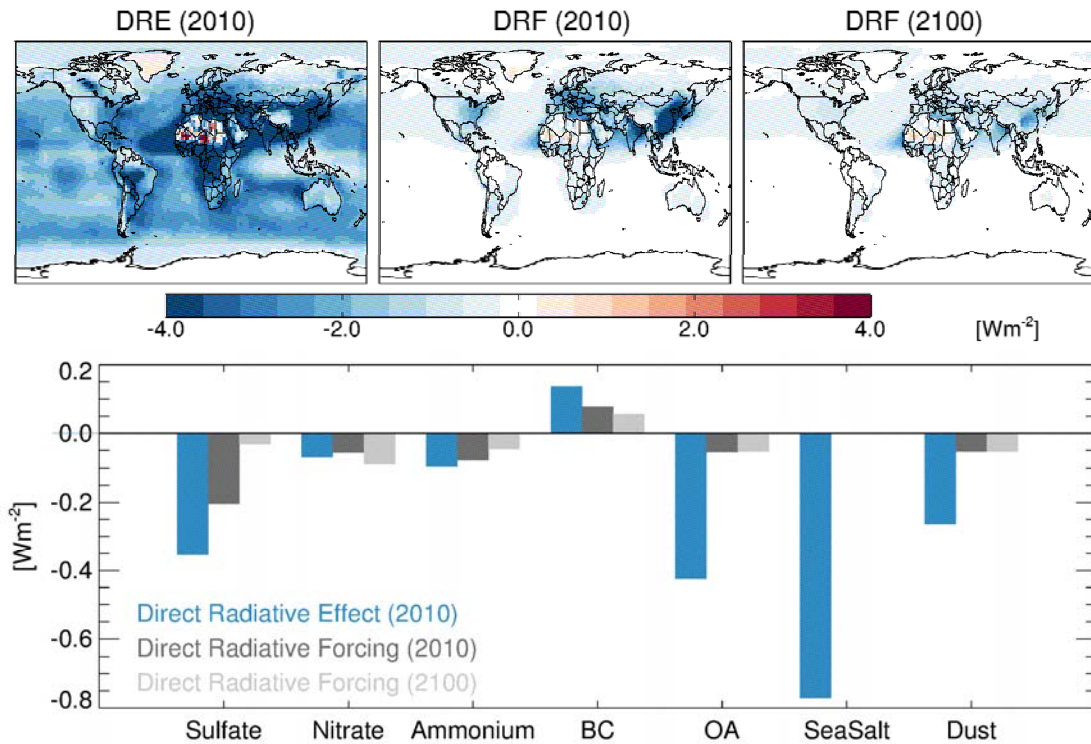


Figure 3. Top: Global annual mean all-sky speciated aerosol TOA Direct Radiative Effect in 2010 (top left, blue), Direct Radiative Forcing for 2010 (top center, dark grey) and Direct Radiative Forcing for 2100 (top right, light grey). Mean values for 2010 are given in Table 3.

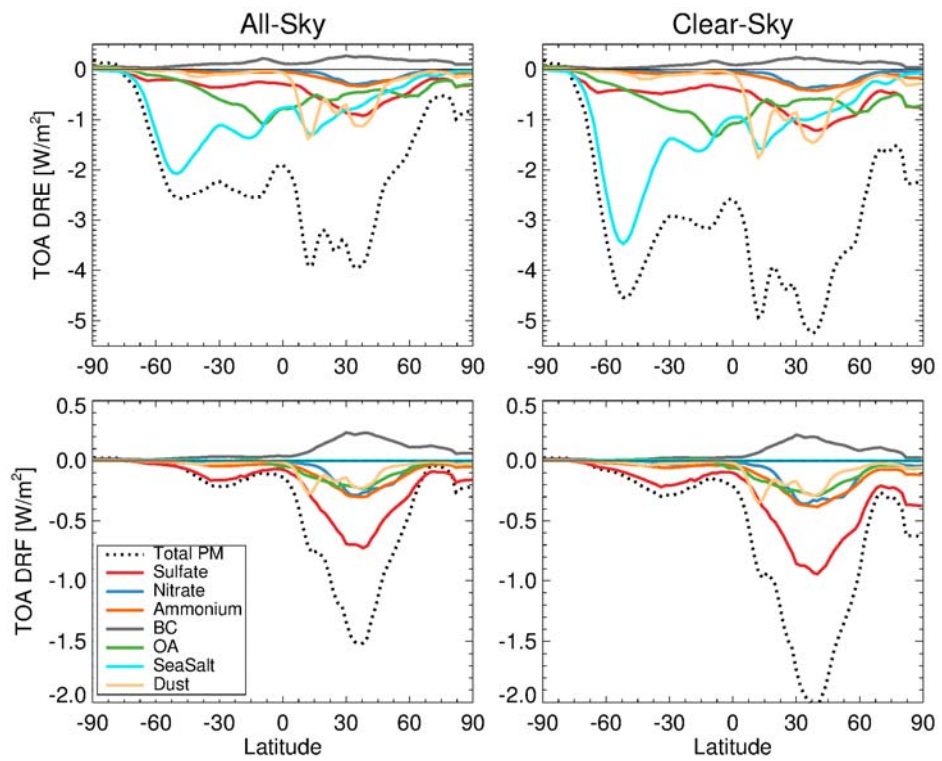


Figure 4. Global zonal mean all-sky speciated aerosol TOA direct radiative effect (top) and direct radiative forcing (bottom) for all-sky (left) and clear-sky (right) simulated by GC-RT for 2010.

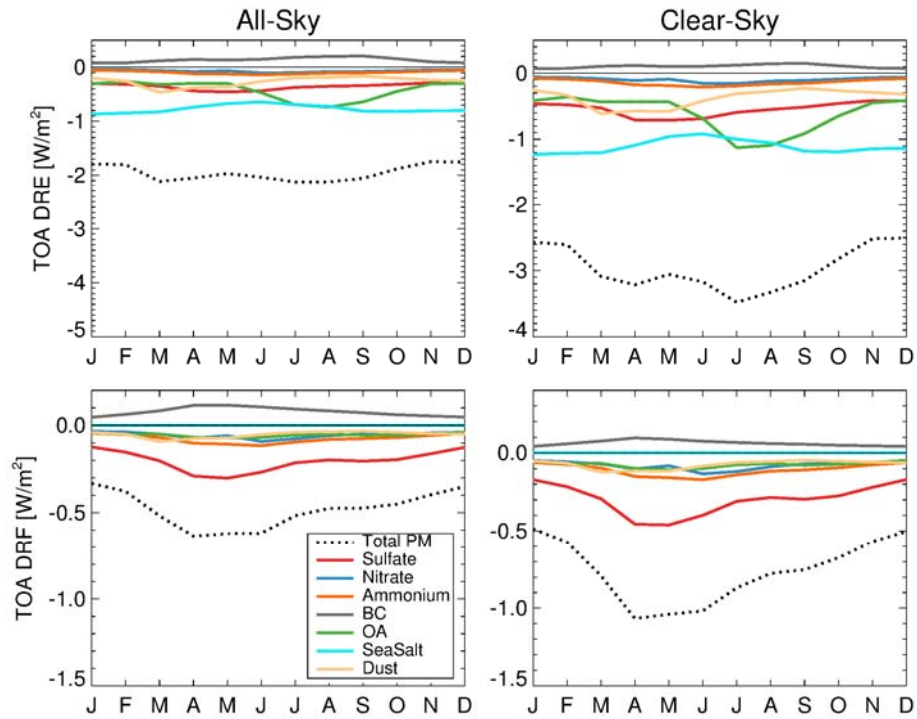


Figure 5. Global seasonal mean speciated aerosol TOA direct radiative effect (top) and direct radiative forcing (bottom) for all-sky (left) and clear-sky (right) simulated by GC-RT for 2010.

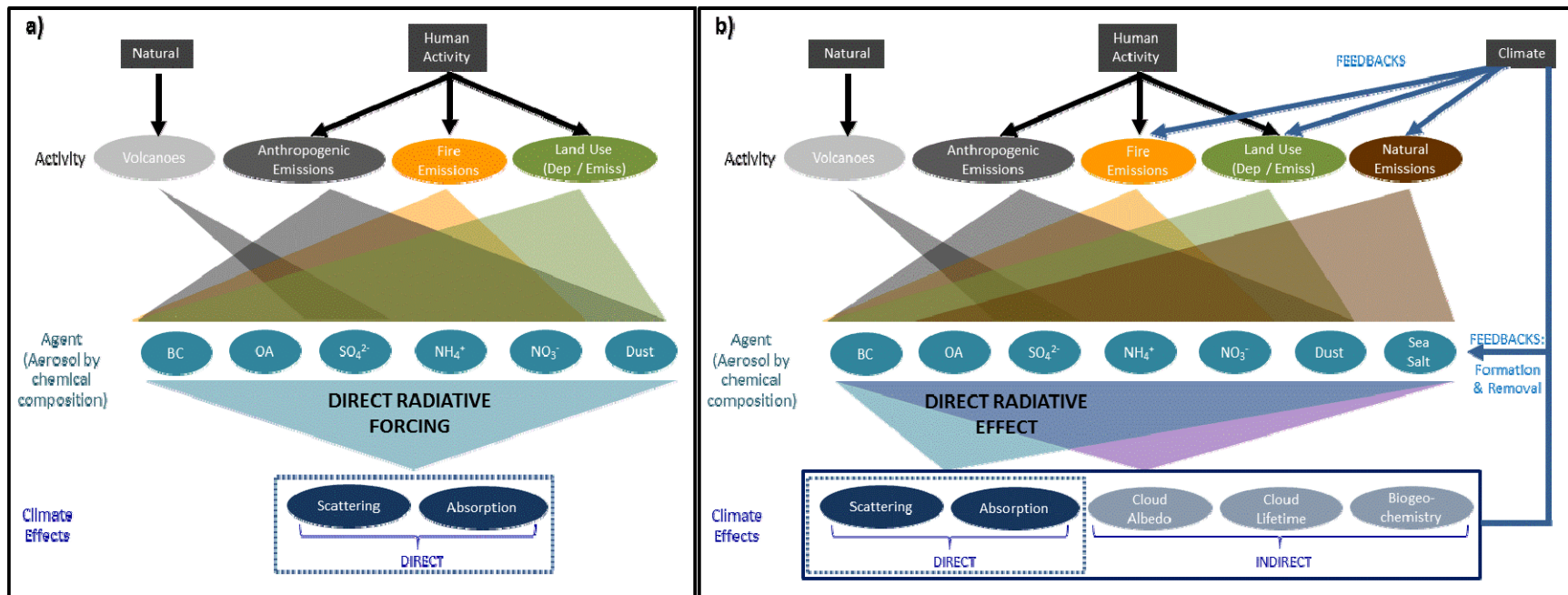


Figure 6. Illustration highlighting the difference between the estimate of a) Direct Radiative Forcing and b) Direct Radiative Effect (right). DRF is the perturbation (since pre-industrial) associated with human activity and natural forcing (i.e. volcanoes). DRE characterizes the instantaneous impact of all aerosols on radiation (including any feedbacks and natural processes).